Series solutions for seepage in three dimensional aquifers

W. W. Read* S. R. Belward P. J. Higgins
G. E. Sneddon

(Received 17 January 2005, revised 3 October 2005)

Abstract

Most models of seepage in homogeneous aquifers assume a two dimensional flow regime. We present a series method that can be used to provide three dimensional solutions for saturated seepage problems in real time. The aquifer lies on a horizontal aquiclude and can have arbitrary soil surface geometry. We show that exponential convergence can be achieved for the correct choice of soil surface representation. The series solutions obtained are used to generate velocity profiles and streamline solutions, once again in real time. These solutions demonstrate the significant differences between two and three dimensional models of seepage.

*Mathematical & Physical Sciences, James Cook University, Townsville, Queensland Australia. mailto:wayne.read@jcu.edu.au

See http://anziamj.austms.org.au/V46/CTAC2004/Read for this article, Published October 21, 2005. ISSN 1446-8735

Contents

1 Introduction **C1127**

2 Mathematical problem description **C1128**

3 Series solution **C1130**
3.1 Evaluation of the series coefficients C1132
3.2 Velocity profiles and streamlines C1133

4 Results **C1134**
4.1 Error analysis C1135
4.2 Velocity and streamline plots C1135

5 Discussion **C1139**

References **C1140**

1 Introduction

The conservation and effective management of subsurface water resources is extremely important, particularly in relatively dry countries like Australia. Quantitative knowledge of the seepage and flow paths through saturated aquifers is crucial in the development of effective management policies. Unfortunately, accurate solutions for the flow field can be extremely difficult to find, even when the soil profile is fully saturated. This problem is exacerbated by the large length to depth ratios common in most practical problems. Consequently, most solution techniques are for two dimensional soil profiles [5]. Although these solutions provide valuable insights into an important class of (simplified) seepage problems, they do not provide any understanding of seepage in genuinely three dimensional aquifers.

Analytic series solutions for the flow equations can be obtained for steady seepage through two dimensional irregular flow domains [1, 2, 3, 4]. Both the potential solution ϕ and the conjugate stream function ψ are immediately available. Unfortunately, for the three dimensional problem, there does not exist a unique stream function formulation, and a number of the powerful features of these techniques are not applicable in this case. However, an analytic series solution can still be obtained for three dimensional seepage using separation of variables. Here we develop a series method for the three dimensional problem, where the soil surface can have arbitrary geometry. We present solutions for the flow field that evince exponential convergence, and use these solutions to derive velocity fields and stream lines. These solutions highlight the difference between two and three dimensional models.

In Section 2, a formal mathematical description of the problem is developed. The series solution method is described in Section 3, followed by the test problem results in Section 4. Finally, the method and results are discussed in Section 5.

2 Mathematical problem description

Consider steady seepage through a homogeneous, saturated aquifer that lies on a horizontal aquiclude with vertical impermeable side boundaries. We non-dimensionalise the problem in terms of the hydraulic conductivity K and the depth d of the aquifer at the origin of the coordinate system. Our non-dimensional variables are $\phi = \phi^*/K$, $x = x^*/d$, $y = y^*/d$ and $z = z^*/d$. A schematic of the flow domain is given in Figure 1.

In the saturated domain, the hydraulic head $\phi(x, y, z)$ satisfies Laplace's equation:

$$\nabla^2\phi = 0\,. \tag{1}$$

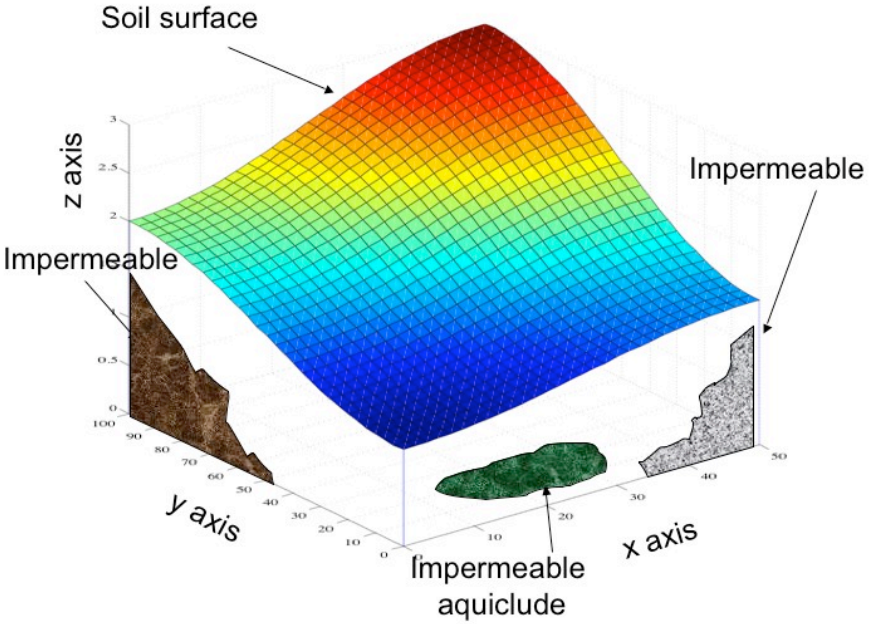

FIGURE 1: Schematic of the flow domain.

Along the impermeable aquiclude $z = 0$, the normal derivative is zero:

$$\frac{\partial}{\partial z}\phi(x, y, 0) = 0\,. \tag{2}$$

On the impermeable, vertical side boundaries $x = 0, s$ and $y = 0, r$, the normal derivatives are also zero:

$$\frac{\partial}{\partial x}\phi(0, y, z) = \frac{\partial}{\partial x}\phi(s, y, z) = \frac{\partial}{\partial y}\phi(x, 0, z) = \frac{\partial}{\partial y}\phi(x, r, z) = 0\,. \tag{3}$$

On the soil surface $z = f^t(x, y)$ (the superscript t indicates the top boundary), the hydraulic head equals the elevation:

$$\phi(x, y, f^t(x, y)) = \phi^t(x, y) = f^t(x, y)\,. \tag{4}$$

3 Series solution

Separation of variables solves Laplace's equation (1). We assume a solution of the form

$$\phi(x, y, z) = X(x)Y(y)Z(z)\,. \tag{5}$$

After substitution into the differential equation, we obtain three ordinary differential equations (ODEs) for $X(x)$, $Y(y)$ and $Z(z)$:

$$X''_\alpha + \alpha^2 X_\alpha = 0\,, \quad Y''_\beta + \beta^2 Y_\beta = 0\,, \quad Z''_\gamma - \gamma^2 Z_\gamma = 0\,, \tag{6}$$

where $\gamma^2 = \alpha^2 + \beta^2$. The eigenvalues α^2 and β^2 are obtained using the homogeneous side boundary conditions

$$X'_\alpha(0) = X'_\alpha(s) = 0\,, \quad Y'_\beta(0) = Y'_\beta(r) = 0\,, \tag{7}$$

with solutions

$$\alpha = m\pi/s\,,\ m = 0, 1, \ldots\,, \quad \beta = n\pi/r\,,\ n = 0, 1, \ldots\,,$$

and the eigenfunctions $X_\alpha(x) = \cos(m\pi x/s)$ and $Y_\beta(y) = \cos(n\pi y/r)$.

The solution to the remaining ODE for Z becomes

$$Z_\gamma(z) = A_\gamma \cosh \gamma z + B_\gamma \sinh \gamma z \,, \tag{8}$$

where

$$\gamma = \pi \sqrt{\frac{m^2}{s^2} + \frac{n^2}{r^2}} \,. \tag{9}$$

Using the bottom boundary condition (2), the series solution is written simply as

$$\phi(x, y, z) = \sum_{m=0}^{\infty} \sum_{n=0}^{\infty} A_{mn} \cos \frac{m\pi x}{s} \cos \frac{n\pi y}{r} \cosh \gamma_{mn} z \,. \tag{10}$$

Using vector space notation, the series solution becomes

$$\phi(x, y, z) = \sum_{m=0}^{\infty} \sum_{n=0}^{\infty} A_{mn} p_{mn}(x, y, z) \,, \tag{11}$$

where

$$p_{mn}(x, y, z) = \cos \frac{m\pi x}{s} \cos \frac{n\pi y}{r} \cosh \gamma_{mn} z \,. \tag{12}$$

In vector space notation, the top boundary condition (4) becomes

$$\phi^t(x, y) = f^t(x, y) = \sum_{m=0}^{\infty} \sum_{n=0}^{\infty} A_{mn} p^t_{mn}(x, y) \,, \tag{13}$$

where

$$p^t(x, y) = p(x, y, f^t(x, y)) \,. \tag{14}$$

The top boundary condition is now used to determine the series coefficients A_{mn} and so define fully the solution for the hydraulic head $\phi(x, y, z)$.

3.1 Evaluation of the series coefficients

We adopt a pseudo spectral approach [6] to evaluate the series coefficients A_{mn}. First, we truncate the series after $m = M-1$, $n = N-1$ terms:

$$\phi_{MN}(x,y,z) = \sum_{m=0}^{M-1}\sum_{n=0}^{N-1} A_{mn} p_{mn}(x,y,z)\,. \tag{15}$$

The top boundary condition (4) now determines the series coefficients. We collocate at $I \times J$ equally spaced collocation points (x_i, y_j), where $i = 0, 1, \ldots, I-1$, $j = 0, \ldots, J-1$, with $x_i = is/(I-1)$ and $y_j = jr/(J-1)$. The top boundary condition (4) becomes

$$\phi^t_{MN}(x_i, y_j) = f^t(x_i, y_j)\,. \tag{16}$$

We write these equations concisely as

$$f^t_{ij} = \sum_{m=0}^{M-1}\sum_{n=0}^{N-1} p_{ijmn} A_{mn}\,. \tag{17}$$

These equations are written in matrix form by transforming m, n, i and j as follows. Letting $k = Mn + m$ and $\ell = Ij + i$, then $k = 0, 1, \ldots, MN-1$, $\ell = 0, 1, \ldots, IJ-1$. The inverse transformations are $n = \lfloor k/M \rfloor$, $m = k - Mn$ and $j = \lfloor \frac{\ell}{I} \rfloor$, $i = \ell - Ij$. Next, let

$$a_k = A_{m,n}, \quad f^t_\ell = f^t(x_i, y_j) \quad \text{and} \quad [\mathrm{P}]_{\ell k} = p_{ijmn}\,. \tag{18}$$

Then, in matrix form, the series coefficients satisfy

$$\mathrm{P}\mathbf{a} = \mathbf{f}^{\mathrm{t}} \tag{19}$$

When $M = N = I = J$, the matrix P is square and can be solved directly, assuming P is nonsingular. When $IJ > MN$ and this is not the case, the discrete least squares approach can be used: $\mathrm{P}^{\mathrm{T}}\mathrm{P}\mathbf{a} = \mathrm{P}^{\mathrm{T}}\mathbf{f}^{\mathrm{t}}$. This reduces (19) to a square system, and can now be solved as before, once again assuming $\mathrm{P}^{\mathrm{T}}\mathrm{P}$ is nonsingular.

3.2 Velocity profiles and streamlines

The velocity distribution $\mathbf{u} = (u, v, w)$ is determined by differentiating the series solution, assuming the new series converges. That is,

$$\mathbf{u} = -\nabla\phi = -\left(\frac{\partial\phi}{\partial x}, \frac{\partial\phi}{\partial y}, \frac{\partial\phi}{\partial z}\right) , \tag{20}$$

and in terms of the series solution

$$u = \frac{\pi}{s}\sum_{m=1}^{\infty}\sum_{n=0}^{\infty} mA_{mn} \sin\frac{m\pi x}{s}\cos\frac{n\pi y}{r}\cosh\gamma_{mn}z\,, \tag{21}$$

$$v = \frac{\pi}{r}\sum_{m=0}^{\infty}\sum_{n=1}^{\infty} nA_{mn} \cos\frac{m\pi x}{s}\sin\frac{n\pi y}{r}\cosh\gamma_{mn}z\,, \tag{22}$$

$$w = -\sum_{m=0}^{\infty}\sum_{n=0}^{\infty} \gamma_{mn}A_{mn} \cos\frac{m\pi x}{s}\cos\frac{n\pi y}{r}\sinh\gamma_{mn}z\,. \tag{23}$$

The streamlines are determined by suitably integrating the velocity field. Given the location (x, y, z) of a fluid particle, the velocity of the particle is

$$(u, v, w) = \left(\frac{dx}{dt}, \frac{dy}{dt}, \frac{dz}{dt}\right) . \tag{24}$$

If we now change to a coordinate ξ, the distance measured along the streamline and positive in the direction of the flow, then

$$\frac{d\xi}{dt} = |\mathbf{u}| = \sqrt{u^2 + v^2 + w^2}\,, \tag{25}$$

and

$$(u, v, w) = \left(\frac{dx}{d\xi}\frac{d\xi}{dt}, \frac{dy}{d\xi}\frac{d\xi}{dt}, \frac{dz}{d\xi}\frac{d\xi}{dt}\right) = |\mathbf{u}|\left(\frac{dx}{d\xi}, \frac{dy}{d\xi}, \frac{dz}{d\xi}\right) . \tag{26}$$

Hence

$$\left(\frac{dx}{d\xi}, \frac{dy}{d\xi}, \frac{dz}{d\xi}\right) = \frac{(u, v, w)}{\sqrt{u^2 + v^2 + w^2}}\,. \tag{27}$$

The autonomous system of ODEs (27) can be solved using standard packages, or integrated directly. For example, consider the x coordinate:

$$x = \int \frac{u}{\sqrt{u^2 + v^2 + w^2}}\, d\xi \,. \tag{28}$$

These integrals are simply approximated using the following scheme. For the streamline passing through (x_i, y_i, z_i), the point $(x_{i+1}, y_{i+1}, z_{i+1})$ estimated by

$$\begin{aligned} (x_{i+1}, y_{i+1}, z_{i+1}) &= (x_i, y_i, z_i) + (\delta x, \delta y, \delta z) \\ &= (x_i, y_i, z_i) + \frac{(u_i, v_i, w_i)}{\sqrt{u_i^2 + v_i^2 + w_i^2}} \delta\xi. \end{aligned} \tag{29}$$

will also lie on this streamline. Obviously the success of this scheme will depend on the size of the increment $\delta\xi$.

4 Results

We examine the effectiveness of this method on the following test problem. We choose $s = 50\,,\ r = 100$ and

$$f^t(x, y) = \left(\frac{(a+1)}{2} - \frac{(a-1)}{2} \cos\frac{\pi x}{s} \right) \left(\frac{(b+1)}{2} - \frac{(b-1)}{2} \cos\frac{\pi y}{r} \right) , \tag{30}$$

with $a = 1.5$ and $b = 2\,.$ The series coefficients are calculated accurately and efficiently using MATLAB, and this software has been used to generate all the results shown in this paper. Figure 1 shows a 21×21 mesh plot of the soil surface.

4.1 Error analysis

The error in the series approximation can be determined by examining the error in the boundary approximations. Note that the only error (in the least squared sense) is due to the truncation error

$$\epsilon_{MN}(x, y, z) = \phi(x, y, z) - \phi_{MN}(x, y, z) \tag{31}$$

in the series approximation, and that this truncation error also satisfies Laplace's equation, due to the choice of basis functions. As Laplace's equation satisfies a maximum principle, the maximum error will occur on the boundary. This error bound is an absolute bound—this bound is one of the most powerful features of the analytic series method.

The root mean squared error ε^t_{MN} for the approximation on the boundary is calculated using

$$\begin{aligned} \varepsilon^t_{MN} &= \left(\frac{\int_0^s \int_0^r \epsilon_{MN}(x, y, f^t(x, y))^2 \, dy \, dx}{\int_0^s \int_0^r dy \, dx} \right)^{1/2} \\ &= \left(\frac{1}{rs} \int_0^s \int_0^r \left(f^t(x, y) - \phi^t_{MN}(x, y) \right)^2 dy \, dx \right)^{1/2}. \end{aligned} \tag{32}$$

This integral can be estimated using quadrature or by discretising the integral using the trapezoidal rule. For the soil profile chosen, Figure 2 shows a log plot of the RMS errors ($\log_{10} \varepsilon^t_{mn}$) versus m and n values ranging from 1 to 20. It is clear from an examination of Figure 2 that the series is converging exponentially to machine precision for $m, n \geq 12$. For $m = n \approx 12$, the series coefficients can be calculated in less than 0.2 seconds on current laptop computers.

4.2 Velocity and streamline plots

The velocity field can be calculated anywhere in the solution domain, at any resolution. Figure 3 shows a plot of the velocity field on the soil surface at

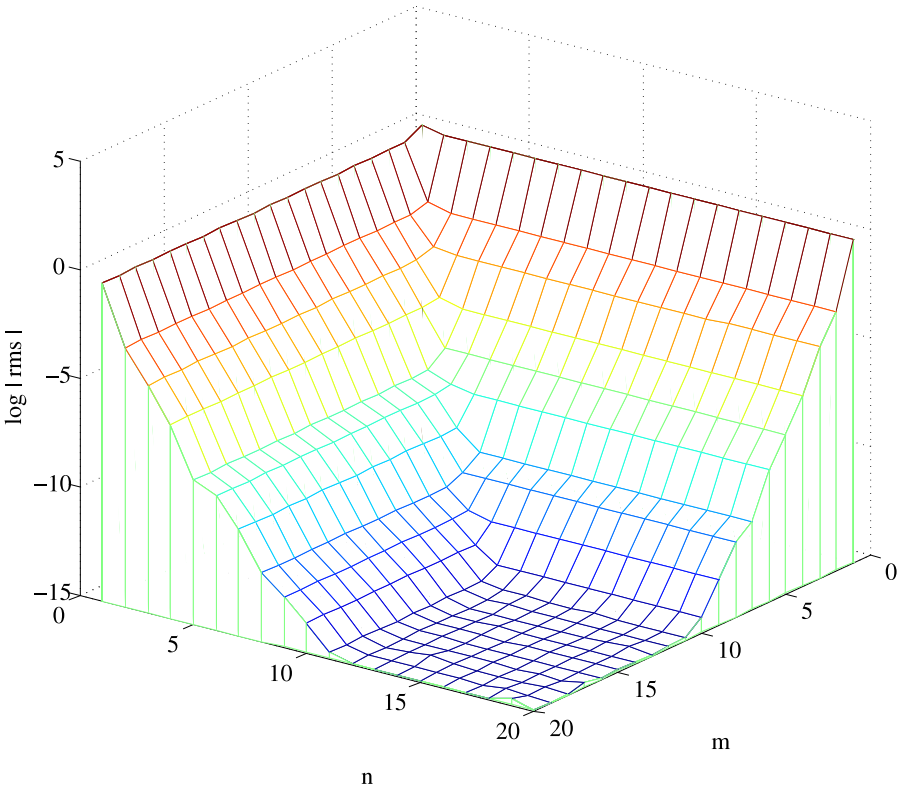

FIGURE 2: Error plot for the test geometry

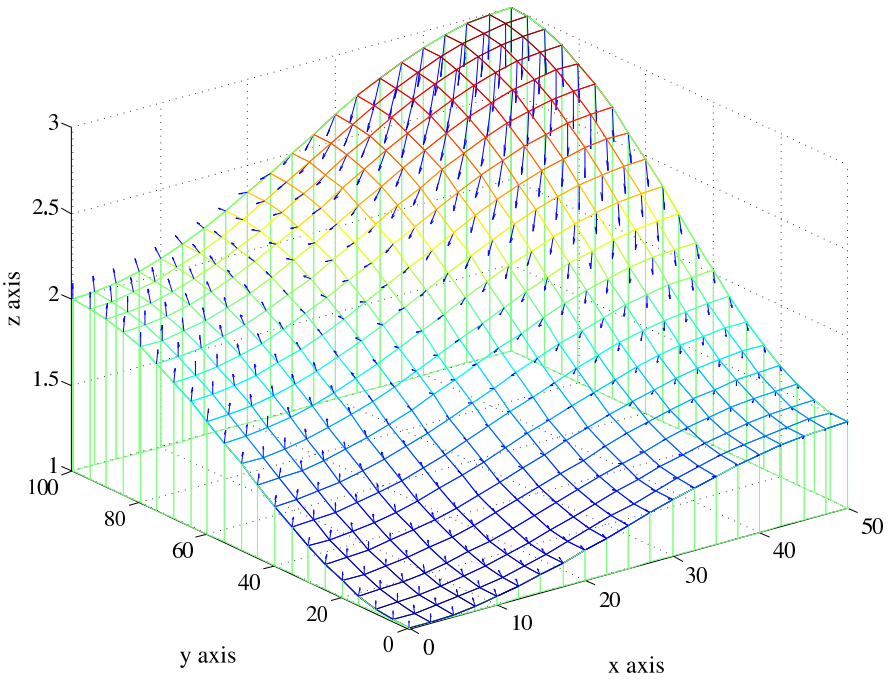

FIGURE 3: Velocity field on the soil surface.

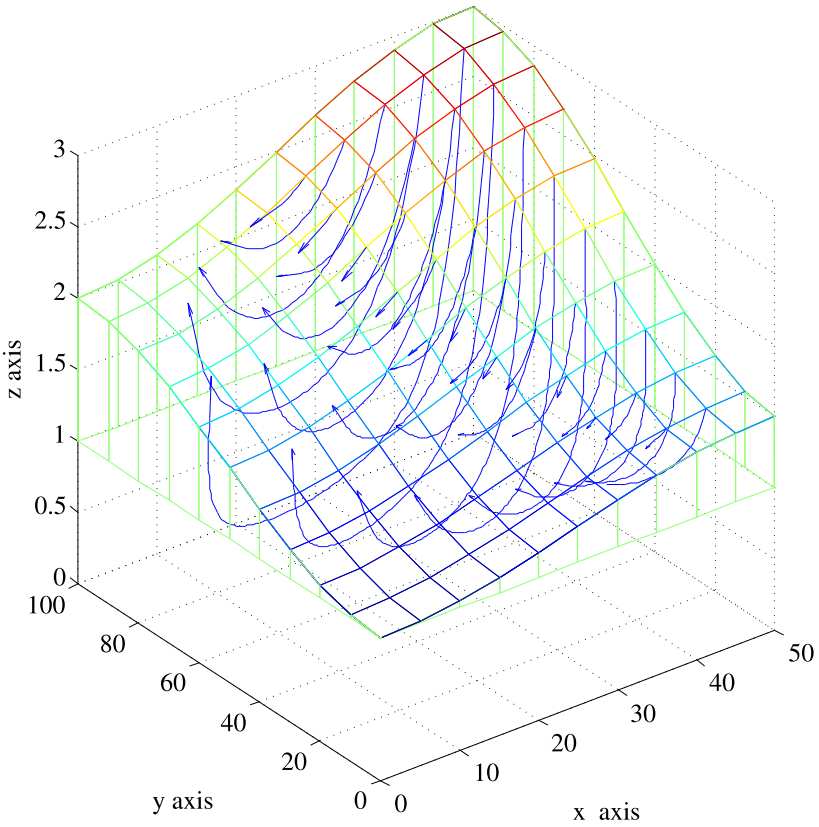

FIGURE 4: Streamlines for the test flow domain.

the mesh plot points in Figure 1. The velocity field on this grid is generated in approximately half a second. Note that fluid enters the hill-slope at $(50, 0, 1.5)$ and seeps from the hill-slope at $(0, 100, 2)$, even though the elevation is higher at this second point.

The streamlines for the test problem have been calculated using the 11×11 mesh grid in Figure 1 and are shown in Figure 4. We chose an 11×11 grid instead of the 21×21 grid so that the streamlines can be clearly seen. However, in this case we have only plotted the streamlines at the mesh points where water is entering the soil—that is, at the upstream mesh points. We also marked the point where the streamline cuts the soil surface when the water is seeping out with an arrow. The streamlines can be calculated using the MATLAB routine ODE43. However, we found that the simple update scheme (29) gave results with similar accuracy when $\delta\xi$ was chosen so that

$$\delta\xi < \frac{\sqrt{s^2 + r^2}}{200}\,. \tag{33}$$

This approach had the advantage of being much more efficient to calculate. Using this approach, the streamline plot presented was calculated in less than 7 seconds on a modern laptop computer (≈ 20 seconds for the 21×21 grid). Note that the streamlines in the plot are genuinely three dimensional and cannot be represented accurately by any two dimensional model.

5 Discussion

We have presented an accurate and very efficient method for solving three dimensional seepage problems. Exponential convergence of the series solution has been achieved, thus providing non-trivial solutions to the partial differential equation that are accurate to machine precision. In addition, these solutions are calculated in real time—less than one second of elapsed time. The velocity field and streamline plots are immediately available, once

again in real time. The solutions for the test problem demonstrate the need for three dimensional models. No two dimensional model would be able to predict flow into an unconfined aquifer below a region where there is outflow!

References

[1] W. W. Read and R. E. Volker, Series solutions for steady seepage through hillsides with arbitrary flow boundaries, *Water Resources Research*, **29**(8) 2871–2880, 1993. http://dx.doi.org/10.1029/93WR00905 C1128

[2] W. W. Read, Series solutions for Laplace's equation with non-homogeneous mixed boundary conditions and irregular boundaries, *Mathematical and Computer Modelling,* **17** 9–19, 1993; http://dx.doi.org/10.1016/0895-7177(93)90023-R Errata, **18** 107, 1993. http://dx.doi.org/10.1016/0895-7177(93)90062-4 C1128

[3] W. W. Read, Hillside seepage and the steady water table I: Theory, *Advances in Water Resources* **19**(2) 63–73, 1996. http://dx.doi.org/10.1016/0309-1708(95)00034-8 C1128

[4] W. W. Read, Hillside seepage and the steady water table II: Applications, *Advances in Water Resources* **19**(2) 75–81, 1996. http://dx.doi.org/10.1016/0309-1708(95)00035-6 C1128

[5] O. D. L. Strack. *Groundwater Mechanics.* Prentice Hall, Englewood Cliffs, New Jersey, 1989. C1127

[6] L. N. Trefethen. *Spectral Methods in MATLAB.* SIAM, Philadelphia, PA, 2000. C1132